1 January 1998

ELSEVIER

Optics Communications 145 (1998) 27–32

OPTICS COMMUNICATIONS

Optimal design of mosaic color filters for the improvement of image quality in electronic endoscopes

Norimichi Tsumura *, Takaya Tanaka, Hideaki Haneishi, Yoichi Miyake

Department of Information and Computer Sciences, Chiba University, Chiba, Japan

Received 7 May 1997; revised 16 July 1997; accepted 28 July 1997

Abstract

A new technique to design mosaic color filters on a CCD area sensor is proposed to improve the quality of electronic endoscope image. Images obtained from the CCD sensor have an interpolation error. The error causes degradation of spatial information in the reproduced image. In this paper, we analyzed spatial distribution of the reflectance spectra in the electronic endoscope image, and the distribution was used to optimize the spectral transmittance of the color filters for the improvement of image quality. The simulated annealing technique was utilized for optimization. © 1998 Elsevier Science B.V.

PACS: 42.30.Va
Keywords: Electronic endoscope; Mosaic color filters; Color reproduction; Simulated annealing

1. Introduction

In recent years, electronic endoscopes with CCD area sensors have been developed and widely used instead of conventional optical endoscopes that use color film. However, color reproduction of the images taken by the electronic endoscope is poor compared with the optical endoscope images. In previous papers [1–3], we proposed color correction methods to colorimetrically correct color using samples of spectral reflectance in gastric mucous membrane. The latest method is based on an estimation of reflectance spectra [2,3]. In the method, the spectral reflectance is estimated in each pixel of the endoscope image, and the estimated spectral reflectance is transformed to the ideal RGB values according to the NTSC system (National Television System Committee) [4]. The estimation and transformation processes are connected then the whole process is performed using simple 3×3 matrix. This method was also proposed for a wide range of images [5].

There are two kinds of color encoding method in electronic endoscopes. One uses a rotating color wheel composed of R, G and B filters in front of the light source. Three channel images are obtained in order, and they are synthesized to be a color image. Moving the probe of the endoscope, however, the color shear is found at the region where the pixel values vary largely, and it prevents correct color reproduction. The other uses mosaic color filters on a CCD sensor to obtain a color image. The captured multiplex image is separated into three channel images where the information is sampled, and these sampled images are filled in by interpolation. In this method, there is no color shear when moving the probe. However, errors by the interpolation prevent the correct color reproduction at the region where the pixel values vary largely.

In this paper [1], we propose a technique to design the color filters to reduce the interpolation error in the electronic endoscope that uses mosaic color filters. The above

* E-mail: tsumura@ics.tj.chiba-u.acjp.

[1] A part of this paper was presented at the 50th Annual Conference of IS&T held in Cambridge, Massachusetts on 21 May 1997.

PII S0030-4018(97)00448-3

color correction method is used as the standard color correction method. The filters are designed based on the two-dimensional distribution of reflectance spectra estimated using the rotating wheel type electronic endoscope without color shear. In the next section, we introduce the color correction method based on the estimation of the reflectance spectra [2,3], and in Section 3, the two-dimensional distribution of estimated reflectance spectra in the electronic endoscope image are analyzed. In Section 4, we show a flowchart for simulation of the image forming process in the electronic endoscope with mosaic color filters, and in Section 5, the spectral transmittance of the filters are optimized by a simulated annealing technique based on the two-dimensional distribution of reflectance spectra.

2. Color correction based on estimated reflectance spectra

Fig. 1 shows a model of the electronic endoscope that uses a rotating color wheel. In this system, the R, G and B values v_i (i = R,G,B) of the electronic endoscope are given by

$$\begin{bmatrix} v_R \\ v_G \\ v_B \end{bmatrix} = \begin{bmatrix} \mathbf{F}_R^t \\ \mathbf{F}_G^t \\ \mathbf{F}_B^t \end{bmatrix} \boldsymbol{o}, \tag{1}$$

where the vector $\boldsymbol{o}$ is a spectral reflectance of the gastric mucous membrane, the vector $\mathbf{F}_i^t$ (i = R,G,B) is the overall spectral characteristic of an electronic endoscope with each filter, and $[\ ]^t$ represents transposition. The over all spectral characteristic is the product of the spectral radiant energy of the light source, spectral characteristics of the imaging lens and CCD sensor, and spectral transmittance of the color filter. Using spectral reflectance data of the gastric mucous membrane, the spectral reflectance $\boldsymbol{o}$ can be well approximated by [2,3]

$$\boldsymbol{o} = [\boldsymbol{u}_1\ \boldsymbol{u}_2\ \boldsymbol{u}_3] \begin{bmatrix} \alpha_1 \\ \alpha_2 \\ \alpha_3 \end{bmatrix}, \tag{2}$$

where $\boldsymbol{u}_i$ is obtained by a principal component analysis of the spectral reflectance data, and the vectors $\boldsymbol{u}_i$ are called principal component vectors. From Eqs. (1) and (2), α_i is given by

$$\begin{bmatrix} \alpha_1 \\ \alpha_2 \\ \alpha_3 \end{bmatrix} = \begin{bmatrix} \mathbf{F}_R^t\boldsymbol{u}_1 & \mathbf{F}_R^t\boldsymbol{u}_2 & \mathbf{F}_R^t\boldsymbol{u}_3 \\ \mathbf{F}_G^t\boldsymbol{u}_1 & \mathbf{F}_G^t\boldsymbol{u}_2 & \mathbf{F}_G^t\boldsymbol{u}_3 \\ \mathbf{F}_B^t\boldsymbol{u}_1 & \mathbf{F}_B^t\boldsymbol{u}_2 & \mathbf{F}_B^t\boldsymbol{u}_3 \end{bmatrix}^{-1} \begin{bmatrix} v_R \\ v_G \\ v_B \end{bmatrix}. \tag{3}$$

From Eqs. (2) and (3), the spectral reflectance is estimated from v_i (i = R,G,B) as follows,

$$\boldsymbol{o} = [\boldsymbol{u}_1\ \boldsymbol{u}_2\ \boldsymbol{u}_3] \begin{bmatrix} \mathbf{F}_R^t\boldsymbol{u}_1 & \mathbf{F}_R^t\boldsymbol{u}_2 & \mathbf{F}_R^t\boldsymbol{u}_3 \\ \mathbf{F}_G^t\boldsymbol{u}_1 & \mathbf{F}_G^t\boldsymbol{u}_2 & \mathbf{F}_G^t\boldsymbol{u}_3 \\ \mathbf{F}_B^t\boldsymbol{u}_1 & \mathbf{F}_B^t\boldsymbol{u}_2 & \mathbf{F}_B^t\boldsymbol{u}_3 \end{bmatrix}^{-1} \begin{bmatrix} v_R \\ v_G \\ v_B \end{bmatrix}. \tag{4}$$

In this paper, we named the two-dimensional distribution of the estimated reflectance spectra as spectral reflectance image. Let the vectors $\boldsymbol{r}$, $\boldsymbol{g}$, $\boldsymbol{b}$ be color matching functions for ideal CRT's display primaries, then R, G, B values v_i' (i = R,G,B) that are obtained by an input system with ideal spectral characteristics are calculated by

$$\begin{bmatrix} v_R' \\ v_G' \\ v_B' \end{bmatrix} = \begin{bmatrix} \boldsymbol{r}^t\boldsymbol{u}_1 & \boldsymbol{r}^t\boldsymbol{u}_2 & \boldsymbol{r}^t\boldsymbol{u}_3 \\ \boldsymbol{g}^t\boldsymbol{u}_1 & \boldsymbol{g}^t\boldsymbol{u}_2 & \boldsymbol{g}^t\boldsymbol{u}_3 \\ \boldsymbol{b}^t\boldsymbol{u}_1 & \boldsymbol{b}^t\boldsymbol{u}_2 & \boldsymbol{b}^t\boldsymbol{u}_3 \end{bmatrix}$$

$$\times \begin{bmatrix} \mathbf{F}_R^t\boldsymbol{u}_1 & \mathbf{F}_R^t\boldsymbol{u}_2 & \mathbf{F}_R^t\boldsymbol{u}_3 \\ \mathbf{F}_G^t\boldsymbol{u}_1 & \mathbf{F}_G^t\boldsymbol{u}_2 & \mathbf{F}_G^t\boldsymbol{u}_3 \\ \mathbf{F}_B^t\boldsymbol{u}_1 & \mathbf{F}_B^t\boldsymbol{u}_2 & \mathbf{F}_B^t\boldsymbol{u}_3 \end{bmatrix}^{-1} \begin{bmatrix} v_R \\ v_G \\ v_B \end{bmatrix}. \tag{5}$$

Eq. (4) shows the estimation process for spectral reflectance, and Eq. (5) shows the total process for color correction using a simple 3×3 matrix.

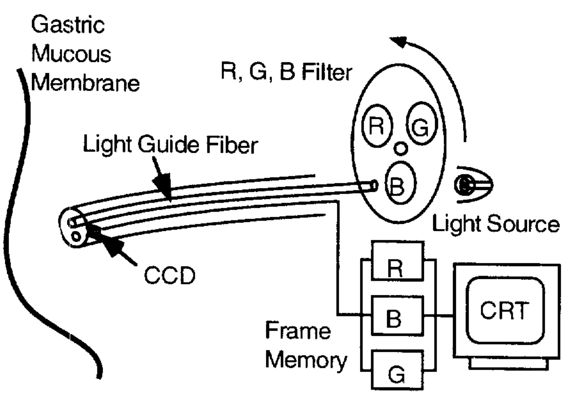

Fig. 1. Model of the electronic endoscope that uses a rotating color wheel.

3. Spatial frequency characteristic of a spectral reflectance image in a gastric mucous membrane

Using the spectral reflectance estimated from the outputs of the rotating wheel type electronic endoscope without color shear, we analyze the spatial distribution of the reflectance spectra in the electronic endoscope image.

For the principle component analysis, we used 310 data of spectral reflectance in the gastric mucous membrane which were measured by an endoscopic spectrophotometer [6]. They were sampled at intervals of 10 nm between 400 and 700 nm. The contribution rate from the first to third components was about 99.1% [3]. We also calculated the contribution rate using 170 reflectance spectra measured by Vrhel et al. [7] which are from various natural and man-made objects, including rocks, plants and vegetation, human skin and hair, and fabrics. The contribution rate was about 97.9%. It is apparent that the reflectance spectra of mucous membrane are better approximated by the three principal components than those of a wide range of objects.

On the other hand, the electronic endoscope image was taken under a Xenon lamp by a rotating wheel type endoscope made by Olympus Optical Co., Ltd. The electronic endoscope image was transformed to spectral reflectance image by Eq. (4) using the individually measured spectral characteristics of the light source, imaging lens, CCD sensor, and color filters.

Fig. 2 shows six slices of the spectral reflectance image at 440, 500, 560, 620 and 680 nm wavelength, and their power spectra in logarithmic scale, respectively. It is noted that the vessel structure can be observed well at the band images from 440 to 560 nm, however it is difficult to observe it at 620 and 680 nm. This characteristic is also obvious in the power spectrums. In the short optical wavelength, the component in high spatial frequency is greater than that in the long optical wavelength. This suggests that the electronic endoscope images should be sampled with higher resolution in the short wavelength to reduce the interpolation error.

4. Image forming simulation in electronic endoscope with mosaic color filters

An image forming process of the electronic endoscope with mosaic color filters is simulated by using the above spectral reflectance image of gastric mucous membrane. The schematic flowchart of the simulation is shown in Fig. 3. The output values on the CCD sensor are calculated using a spectral reflectance image and the overall spectral characteristic of an electronic endoscope using Eq. (1). The overall spectral characteristic in the previous section was used as the characteristic for simulation. The output value of each pixel depends on the spectral transmittance of the color filter. The output values are separated into three channel images and these sampled images are interpolated. The interpolated three channel images are transformed to R, G and B images that are obtained by an input system with ideal spectral sensitivities using our proposed color correction method [2,3] as in Eq. (5). Bayer type [8] color filter array was used as a mosaic pattern on the CCD sensor. The primary color obtained by the third filter is sampled with higher resolution than the others. In this paper, we have not considered other mosaic patterns (see Ref. [9]) and have not optimized the mosaic pattern. The reason for this procedure is discussed in Section 6.

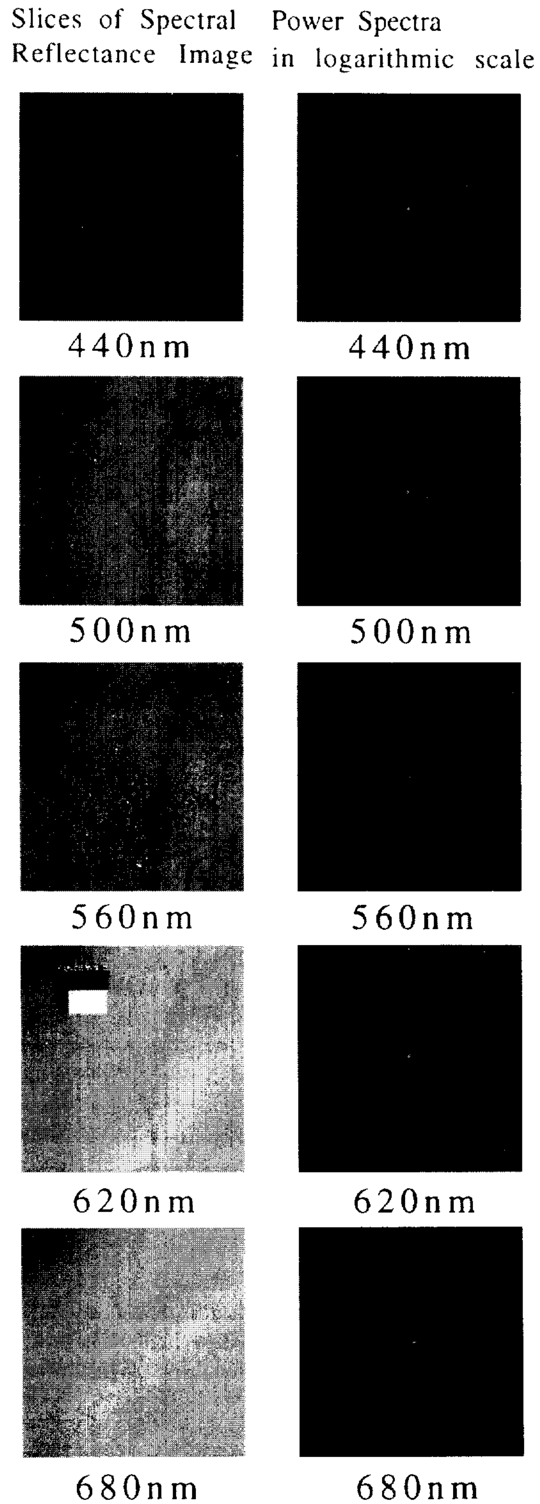

Fig. 2. Slices of spectral reflectance image at 440, 500, 560, 620 and 680 nm wavelength, and their power spectra in logarithmic scale.

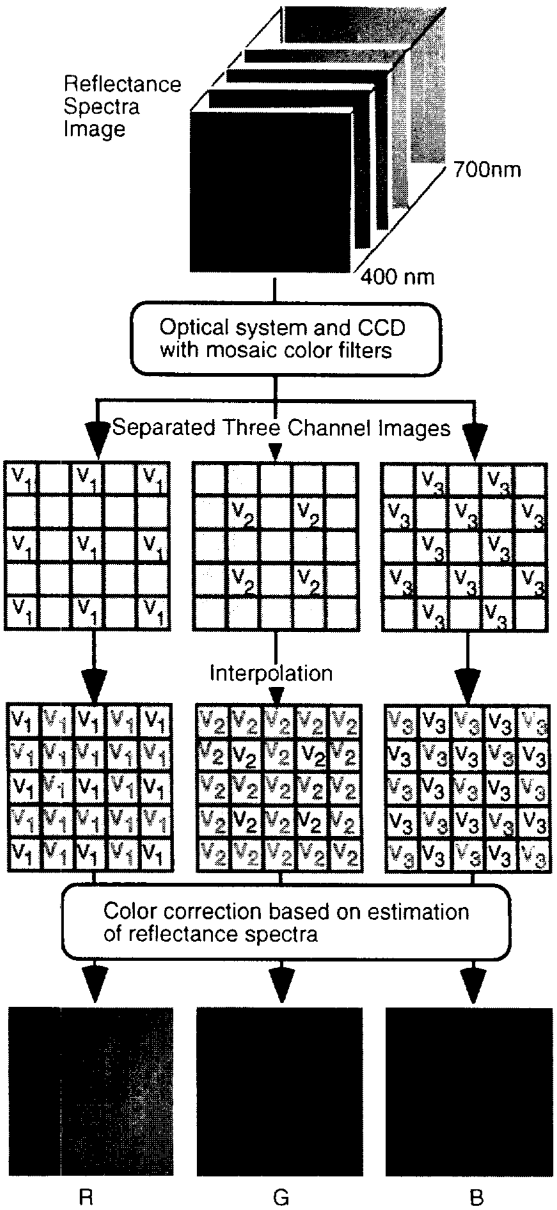

Fig. 3. Schematic flowchart of simulation for the electronic endoscope with mosaic color filters using a spectral reflectance image of the gastric mucous membrane.

We considered that both characteristics of sampling and spectral reflectance image should be used to improve the image quality. In the next section, we design the mosaic color filters for this purpose.

5. Design of filter spectral transmittance by simulated annealing

The color filters were designed to minimize an averaged color difference in CIE L^* a^* b^* uniform color space [10] of all pixels between the original image and the sampled-interpolated image. We used only normal formulae [10] in CIE L^* a^* b^* uniform color space to compute the color differences at high speed. As a preliminary research for optimization, in this paper, we treated only one typical spectral reflectance image shown in Fig. 2. The simulated annealing method [11] that is one of the nonlinear optimization techniques was used to find the color filters that minimize the averaged color difference as a cost function. We assumed that the filters have Gaussian type transmittance curves. As parameters in the optimization, the spectral centroid and half-width of Gaussian type were used, then six parameters for three filters were optimized in this paper. Gaussian noise was added into sensor outputs as electronic noise. The degree of noise is denoted by the ratio between the standard deviation of noise and the output value for perfectly reflecting surface without color filters.

Fig. 4 shows the optimized spectral transmittance of

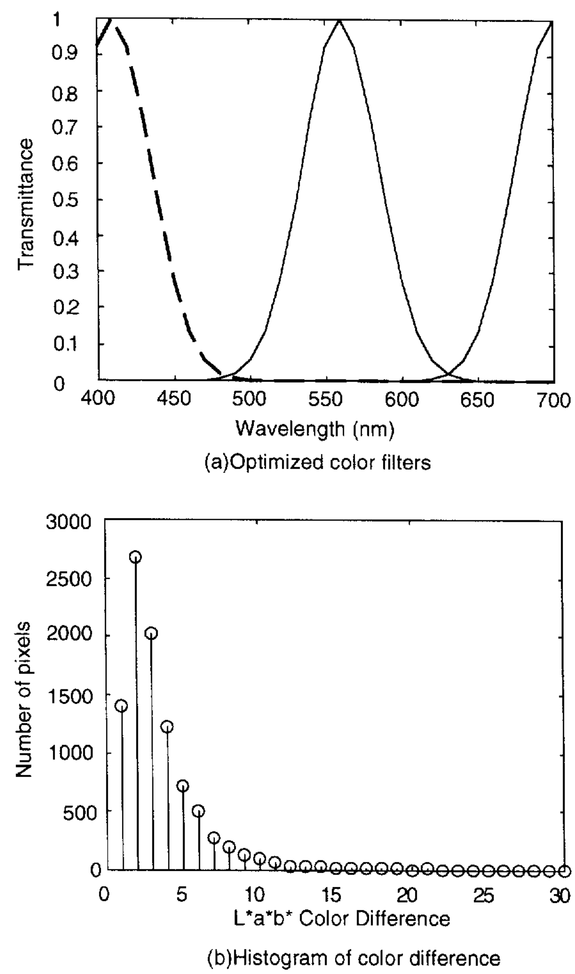

Fig. 4. Optimized color filters in the presence of 0.1% noise (a) spectral transmittance of color filters, and (b) histogram of CIE L^* a^* b^* color difference.

color filters in the presence of 0.1% noise and the histogram of CIE L* a* b* color difference between the original image and processed image. The dashed line in Fig. 4 indicates the spectral transmittance of the third filter. The average and maximum color differences were 6.7 and 176.3 respectively. To examine the result of the optimization, other color filters are shown in Fig. 5a and a result of color difference is shown in Fig. 5b as a histogram. The average and maximum color differences were 10.1 and 197.5, respectively. The half-widths of the color filters were set to be the same as the optimized color filters, but their centroids were shifted. In general, it is known that the just noticeable color difference is about 2.5 in CIE L* a* b* color space. We can see that the color filters are optimized effectively by suppressing color differences of many pixels within 2.5 under the histograms, and we can conclude that both characteristics of the spectral reflectance image and the sampling process cooperate with each other to improve the image quality.

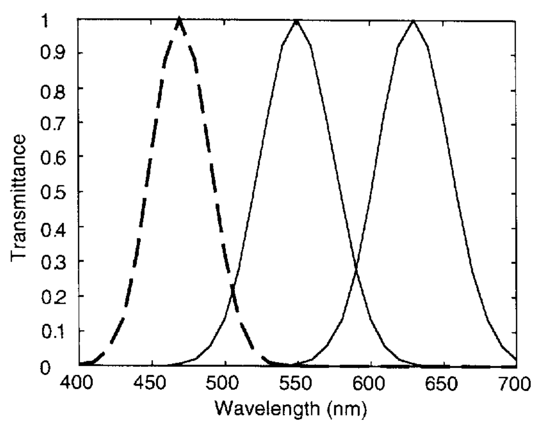

(a)Examined color filters

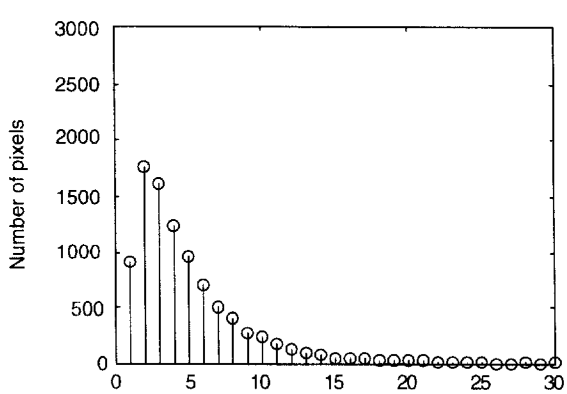

(b)Histogram of color difference

Fig. 5. Examined color filters in the presence of 0.1% noise (a) spectral transmittance of color filters, and (b) histogram of CIE L* a* b* color difference.

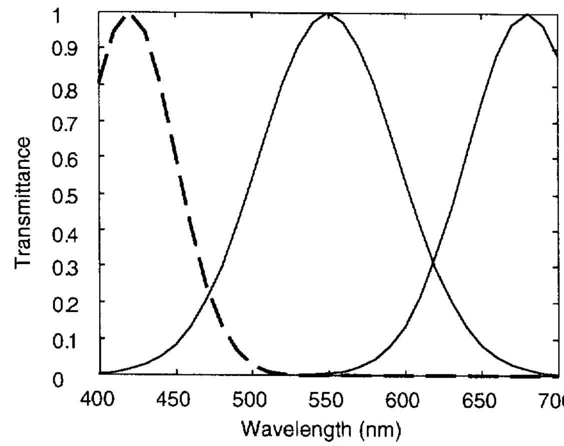

(a)Optimized color filters

Fig. 6. Optimized color filters in the presence of 0.5% noise.

In the presence of 0.5% noise, the half-widths of the optimized color filters become larger than those in Fig. 4 as shown in Fig. 6. This is because the sensor outputs of the narrow band filters become smaller and are more strongly influenced by noise than those of the wide band filters, that is the half-width of the optimized filters become larger as the degree of noise becomes stronger. In a practical situation, it is necessary to estimate the degree of noise in the optimization of color filters.

6. Discussion

In this paper, the spectral transmittance of color filters was optimized on a Bayer type mosaic pattern to improve the image quality. The mosaic pattern can be also optimized to improve the image quality. However, it is difficult to adjust the sampling rate finely by changing the mosaic pattern owing to the restriction of the filters arrangement and interpolation technique. Therefore, we have not optimized the mosaic pattern, and expected that the spectral transmittance is optimized to cooperate with the sampling rates of the Bayer pattern.

We approximated the spectral reflectance by using three principal components. The cumulative contribution ratio of the three principal components was about 99%. The error of this approximation is often enlarged at the resultant image depending on the relation between the principal component vectors and spectral transmittance vectors [5]. In our simulation, this enlargement of the approximation error could not be considered, because our spectral reflectance image was expressed by only three principal components exactly. We should use three more color filters in the rotating wheel type electronic endoscope to obtain a more exact spectral reflectance image.

Some techniques [12–15] have been proposed to design color filters for color measurement devices using a linear iterative technique or a constrained nonlinear optimization. It was not necessary to consider the reproduction of the spatial distribution of the image, because there was not any interpolation error in their applications. In our application, however, we had to consider the degradation by the interpolation error for the design of mosaic color filters, and a spectral reflectance image was required to simulate an image forming process and calculate the cost function for optimization. The simulated annealing technique was useful for this application because the cost function is complicated by the processes of sampling, interpolating and correcting of color, and we can easily add other costs such as feasibility of filter fabrication.

These ideas have been discussed in the context of a specific application of an electronic endoscope that uses mosaic color filters. The new concept for designing the optimum filter considering both characteristics of the spectral reflectance image and the sampling process is extremely general for the applications where mosaic color filters are used and objects have a remarkable characteristic of the spectral reflectance image.

7. Conclusion

We proposed a technique to design mosaic color filters of an electronic endoscope to improve image reproduction. The filters were designed with reflectance spectra estimated form the RGB image acquired by a rotating wheel type electronic endoscope without color shear. We found that complex structures as a vessel pattern appear in short wavelength slices of the spectral reflectance image. The simulated annealing method was used to find the color filters that minimize the averaged color difference between original images and sampled-interpolated images. The result of the optimization showed that the characteristic of the sampling and spectral reflectance image cooperated well with each other to improve the image quality.

Acknowledgements

A portion of this study was supported by a Grant-in-Aid for Science Research (No. B08455031) by the Japanese Ministry of Education.

References

[1] H. Haneishi, T. Shiobara, Y. Miyake, Optics Comm. 114 (1995) 57.
[2] T. Shiobara, S. Zhou, H. Haneishi, Y. Miyake, Proc. of the IS&T/SID 1995 Color Imaging Conf., 1995, p. 186.
[3] T. Shiobara, S. Zhou, H. Haneishi, N. Tsumura, Y. Miyake, J. Imaging Sci. Technol. 40 (1996) 494.
[4] R.W.G. Hunt, The Reproduction of Colour, 5th ed., Fountain Press, 1995.
[5] M.J. Vrhel, H.J. Trussell, Color Res. Appl. 17 (1992) 328.
[6] Y. Miyake, T. Sekiya, T. Yano, S. Kubo, T. Hara, J. Photogr. Sci. 37 (1989) 134.
[7] M.J. Vrhel, R. Gershon, L.S. Iwan, Color Res. Appl. 19 (1994) 4–9.
[8] B.E. Bayer, US Patent 3,971,065 (1976).
[9] M.A. Kriss, Proc. of IS&T's 49th Annu. Conf., 1996, p. 272.
[10] G. Wyszecki, W.S. Stiles, Color Science: Concepts and Methods, Quantitative Data and Formulae, Wiley, New York, 1982, p. 167.
[11] S. Kirkpatrick, C.D. Gelatt Jr., M.P. Vecchi, Science 220 (1983) 671.
[12] M.J. Vrhel, H.J. Trussell, J. Bosch, J. Electron. Imaging 4 (1995) 6.
[13] M.J. Vrhel, H.J. Trussell, IEEE Trans. Image Process. 3 (1994) 147.
[14] M. Wolski, C.A. Bouman, J.P. Allebach, E. Walowit, IEEE Trans. Image Process. 5 (1996) 507.
[15] P.L. Vora, J. Trussell, IEEE Trans. Image Process. 6 (1997) 312.